MULTIPLE CHANGE POINT DETECTION BASED ON HODRICK-PRESCOTT AND l_1 FILTERING METHOD FOR RANDOM WALK TIME SERIES DATA

A PREPRINT

Xiyuan Liu
Department of Mathematics and Statistics
Louisiana Tech University, Ruston, LA
liuxyuan@latech.edu

ABSTRACT

We propose new methods for detecting multiple change points in time series, specifically designed for random walk processes, where stationarity and variance changes present challenges. Our approach combines two trend estimation methods: the Hodrick–Prescott (HP) filter and the l_1-filter. A major challenge in these methods is selecting the tuning parameter λ, which we address by introducing two selection techniques. For the HP-based change point detection, we propose a probability-based threshold to select λ under the assumption of an exponential distribution. For the l_1-based method, we suggest a selection strategy assuming normality. Additionally, we introduce a technique to estimate the maximum number of change points in time segments using the l_1-based method. We validate our methods by comparing them to similar techniques, such as PELT, using simulated data. We also demonstrate the practical application of our approach to real-world SNP stock data, showcasing its effectiveness in detecting change points.

Keywords Data segmentation; trend estimation; change point detection; random walk

1 Introduction

This article introduces a novel methodology for detecting multiple change points in time series data, leveraging two trend estimation methods: the Hodrick–Prescott (HP) filter and the l_1-filter (Kim et al., 2009), a piecewise non-parametric linear model. The proposed approach is particularly well-suited for analyzing random walk time series. A key challenge in these Lagrange multiplier-based applications—the selection of the tuning parameter λ—is effectively addressed through the proposed methodology. Additionally, the HP filter-based change point detection method constructs an α-level time segment under the Poisson process assumption, while the l_1-filter-based method estimates the maximum number of change points within given time segments. This section reviews existing techniques for multiple change point detection and trend estimation, highlighting their extensions and demonstrating their effectiveness in identifying complex change point patterns in time series data.

A common approach to change point detection involves applying hypothesis testing sequentially over time, as exemplified by methods like Cumulative Sum (CUSUM) (Csörgö and Horváth, 1997) and Moving Sum (MOSUM) (Kim et al., 2024). These techniques are particularly effective for identifying change points in time series that are stationary or exhibit linear trends with independent errors. However, their accuracy diminishes when applied to random walk time series, where stationarity and changes in variance poses significant challenges. A potential solution to this issue is to estimate the autocorrelation function of the series and utilize it to determine an appropriate lag. The modified time series can then be analyzed using these methods, improving their applicability and performance in the context of random walks (Sun et al., 2008; Chan and Yau, 2017).

An alternative strategy focuses on estimating a latent function corresponding to the time variable from the observed time series—commonly referred to as trend estimation—and subsequently applying hypothesis testing to detect change points (Cho and Fryzlewicz, 2024). Singular Spectrum Analysis (SSA) is a prominent method for trend estimation

within this framework (Vautard and Ghil, 1989; Broomhead et al., 1987; Broomhead and King, 1986; Poskitt, 2020). It achieves this by transforming the time series into a trajectory matrix and applying Principal Component Analysis (PCA) to decompose the matrix into a linear combination of elementary matrices, effectively extracting the latent function. Following this, a typical approach for applying CUSUM involves creating a base matrix window from the observed time series and using the distance between future time series values and the base matrix as a statistic for hypothesis testing to detect change points (Moskvina and Zhigljavsky, 2003; Alanqary et al., 2021).

Another approach within this strategy involves minimizing an objective function that incorporates both a cost function and a penalty function to avoid overfitting. A commonly used cost function in this context is the negative log-likelihood (Chen et al., 2000), with the Pruned Exact Linear Time (PELT) method being a popular example (Killick et al., 2012).

Our proposed method builds on this framework by leveraging two well-known trend estimation techniques from economics: the HP filter and the l_1-filter. These methods are used as objective functions, followed by hypothesis testing (for the HP filter) or a thresholding approach (for the l_1-filter) to determine the number of change points. Each method is suited to different scenarios: the HP filter can construct an α-level confidence interval for detecting change points within time intervals, while the l_1-filter achieves a lower false discovery rate and estimates the total number of change points more accurately. Since both methods are used for trend estimation, we begin by introducing the background and significance of trend estimation in this context.

1.1 Trend estimation

Numerous methods are available to detect the latent function, or long-term trend effects, including moving average filters (Golestan et al., 2013), smoothing splines (Wang, 1998),and the Principle Component Analysis (PCA) approach (Li et al., 2015). One popular non-parametric approach is the HP filter, which is widely utilized in economics for trend extraction (De Jong and Sakarya, 2016).

1.1.1 HP-filter

Let

$$y_t = x_t + \epsilon_t, \quad t = 0, 1, ..., T$$

where y_t is the observed time series data, x_t is the underlying trend, and $\epsilon_t \overset{i.i.d.}{\sim} N(0, \sigma^2)$ is the random error at time t with mean zero and finite variance σ^2; the HP filter estimates x_t by finding the $\hat{x}_t$ such that

$$\hat{x}_t = \underset{x_t \in \mathbb{R}}{\operatorname{argmin}} \left[(1/2) \sum_{t=0}^{T} (y_t - x_t)^2 + \lambda \sum_{t=1}^{T-1} (x_{t-1} - 2x_t + x_{t+1})^2 \right],$$

where $\lambda > 0$ is a tuning parameter. If we let $\mathbf{y} = (y_0, y_1, ..., y_T) \in \mathbb{R}^{T+1}$, $\mathbf{x} = (x_0, x_1, ..., x_T) \in \mathbb{R}^{T+1}$, then the objective function above can be rewritten as

$$\hat{\mathbf{x}} = \underset{\mathbf{x} \in \mathbb{R}^{T+1}}{\operatorname{argmin}} \left[(1/2) \|\mathbf{y} - \mathbf{x}\|_2^2 + \lambda \|\mathbf{D}\mathbf{x}\|_2^2 \right], \tag{1}$$

where

$$\mathbf{D}_2 = \begin{bmatrix} 1 & -2 & 1 & & & \\ & 1 & -2 & 1 & & \\ & & \ddots & \ddots & \ddots & \\ & & & 1 & -2 & 1 \end{bmatrix}.$$

In Eq. (1), $\|\mathbf{u}\|_2 = (\sum u_t^2)^{1/2}$ is the l_2 norm, and $\mathbf{D}_2 \in \mathbb{R}^{(T-1)\times(T+1)}$ is the second-order difference matrix.

While the HP filter offers a notable advantage in filtering out short-term errors and depicting the long-term trend, Hamilton (2018) highlights a limitation: the filter cannot accurately capture the actual data-generating process.

1.1.2 l_1-filter

Instead of using the Lagrange multiplier with the l_2 norm, l_1 trend filtering employs the l_1 norm Kim et al. (2009), that is

$$\hat{\mathbf{x}} = \underset{\mathbf{x} \in \mathbb{R}^{T+1}}{\operatorname{argmin}} \left[(1/2) \|\mathbf{y} - \mathbf{x}\|_2^2 + \lambda \|\mathbf{D}_2\mathbf{x}\|_1 \right], \tag{2}$$

where $\|\mathbf{u}\|_1 = \sum |u_t|$. A key advantage of using the l_1 norm as the penalty function, rather than the l_2 norm, is that it naturally enforces a piecewise linear regression structure. This assumes that the trend can be modeled as

$$x_t = \alpha_k + \beta_k t, \quad t_{k-1} \leq t \leq t_k, \quad k = 1, 2, ..., K,$$

where $0 = t_0 < t_1 < \cdots < t_{K-1} < t_K = T$, and $t_1, t_2, \ldots, t_{K-1}$ represent the change points. In l_1 filtering, the change points are treated as kink points. For instance, if t_k is a the change point between $[t_{k-1}, t_k]$ and $[t_k, t_{k+1}]$, the model enforces the continuity condition

$$a_{k-1} + \beta_{k-1} t_k = a_k + \beta_k t_k.$$

This makes l_1 trend filtering particularly well-suited for data that follow a piecewise linear regression structure, a common assumption in economics. However, similar to the HP filter, l_1 trend filtering uses the Lagrange multiplier λ as a penalty parameter, which requires careful tuning based on the researcher's expertise. If λ is too small, the filter may identify every observed data point as a change point. Conversely, if λ is too large, critical change points may be overlooked.

The remainder of this paper is organized as follows: Section 2 provides a detailed explanation of how both HP filtering and l_1 filtering are applied to identify change points. Section 3 outlines the steps for conducting a normality test to eliminate λ for both HP and l_1 filtering. Section 4 introduces two gradient descent-based optimization methods for determining the optimal value in l_1 filtering. Section 5 presents numerical experiments to demonstrate the effectiveness of our change point detection approach using both HP and l_1 filtering. Finally, Section 6, we apply the proposed method to S&P 500 data from Yahoo Finance as a case study.

2 Change point detection model

2.1 Model assumption

We define y_t be the observed time series with $t = 0, 1, ..., T$ time points, and K segments (i.e., $0 = t_0 < t_1 < \cdots < t_{K-1} < t_K = T$, $K-1$ change points) such that

$$y_0 = \epsilon_0, \quad y_t = \sum_{k=1}^{K} \beta_k [I(t_{k-1} < t < t_k)] + y_{t-1} + \epsilon_t, \quad t = 1, 2, ..., T, \tag{3}$$

where β_k is the constant parameter in the segment k, $I(\cdot)$ is the indication function such that

$$I(t_{k-1} < t < t_k) = \begin{cases} 0, & t \notin (t_{k-1}, t_k) \\ 1, & t \in (t_{k-1}, t_k), \end{cases} \quad k = 0, 1, ..., K-1,$$

and $\epsilon_t \overset{i.i.d.}{\sim} N(0, \sigma^2)$ is the error term with mean zero and variance σ^2. We employ this model form under the assumption that the current position at time t is influenced by three factors: the drifted (β_k) that causes long-term motion within the time segment k, the position at the previous time step (y_{t-1}), and the unobserved errors (ϵ_t) arising from other environmental factors. Furthermore, we assume that the drift remains consistent only within specific time segments ($I(t_k < t < t_{k+1})$). Based on these assumptions, we establish the relationship between the observed time series $\{y_t\}_{t=0}^T$ and the expected time series $\{x_t\}_{t=0}^T$ as outlined in the following assumption.

Assumption 1. *Let $\{y_t\}_{t=0}^T$ be a sequence of random variables defined as follows:*

$$y_t = \begin{cases} \epsilon_t & \text{if } t = 0, \\ y_t = x_t + \epsilon_t & \text{if } t = 1, 2, ..., T, \end{cases}$$

where $\{\epsilon_t\}_{t=0}^T \overset{i.i.d.}{\sim} N(0, \sigma^2)$. The noise ϵ_t satisfies $E(\epsilon_t) = 0$, and $Var(\epsilon_t) = \sigma^2 < \infty$.

Assumption 1 is directly linked to the first part of Eq. (1) and Eq. (2) as the first parts for both equations uses l_2 norm to measure the distance between $\{y_t\}_{t=0}^T$ and $\{x_t\}_{t=0}^T$. This assumption ensures that, with an appropriate choice of λ, and under the condition that the time series contains additive error, the error term follows a normal distribution. Consequently, we can assess the accuracy of our λ value by conducting hypothesis testing on the error terms using a normality test. In this paper, we employed the Shapiro-Wilk normality test due to its higher statistical power compared to other methods (Razali et al., 2011).

Although l_1-filter is the most suitable model under this assumption, its use of l_1 norm as a penalty makes it relatively difficult to derive the Least Squares Estimate (LSE) and perform statistical inference. Therefore, we begin with the HP-based change point detection method, which is more straightforward for making inferences, and then extend this approach to the l_1-based method.

2.2 HP-based change point detection

Based on the definition of the HP filter, we estimate $\mathbf{y}$ using the Least Squared Estimate (LSE) with a penalty function generated by the Lagrange multiplier. The loss function for the LSE is defined as:

$$l_{HP}(\mathbf{x}) = (1/2)\|\mathbf{y} - \mathbf{x}\|_2^2 + \lambda\|\mathbf{D}_2\mathbf{x}\|_2^2, \tag{4}$$

where $\lambda \in [0, +\infty)$ is the tuning parameter, $\mathbf{D}_2 \in \mathbb{R}^{(T-1)\times(T+1)}$ is the second-order difference matrix defined above, $\mathbf{y} = \{y_t\}_{t=0}^T$ is the observed data vector, and $\mathbf{x} = \{x_t\}_{t=0}^T$ represents the expected time series.

By the Lagrangian duality, solving Eq. (4) is equivalent to solving the following optimization problem.

$$\begin{aligned} &\underset{\mathbf{x}\in\mathbb{R}^T}{\text{minimize}} \left\{(1/2)\|\mathbf{y} - \mathbf{x}\|^2\right\} \\ &\text{subject to } \|\mathbf{D}_2\mathbf{x}\|_2^2 \le m, \end{aligned} \tag{5}$$

where $m > 0$ and the Lagrange multiplier λ in Eq. (1) is negatively correlated to the value of m. Based on this, we can then introduce the following assumptions.

Assumption 2. *There exists a constant $m \in (0, \infty)$ such that the following smoothness condition holds for the expected time series, $\{x_t\}_{t=0}^T$.*

$$\|\mathbf{D}_2\mathbf{x}\|_2^2 = \sum_{t=2}^{T}(x_{t-1} - 2x_t + x_{t+1})^2 \le m.$$

Assumption 2 is specifically designed for the second term in the loss function Eq. (4). As a result, the LSE for Eq. (4) is equivalent to the solution for Eq. (5) under Assumptions 1 and 2.

Since Eq. (4) is convex, the estimate of $\mathbf{y}$ can be obtained by taking the gradient of Equation (4) with respect to $\mathbf{x}$ and setting it equal to zero. This yields the LSE of $\mathbf{y}$ for the HP filter:

$$\hat{\mathbf{x}}^{HP} = (\mathbf{I}_{T+1} + 2\lambda\mathbf{D}_2^T\mathbf{D}_2)^{-1}\mathbf{y},$$

where $\mathbf{I}_{T+1} \in \mathbb{R}^{(T+1)\times(T+1)}$ is the identity matrix. Consequently, the estimated error is

$$\mathbf{e}^{HP} = \left(\mathbf{y} - \hat{\mathbf{x}}^{HP}\right) = 2\lambda(\mathbf{I}_{T+1} + 2\lambda\mathbf{D}_2^T\mathbf{D}_2)^{-1}\mathbf{D}_2^T\mathbf{D}_2\mathbf{y}. \tag{6}$$

With the model assumptions 1 and 2, if there is no change point in the data, then

$$(y_{t-1} - 2y_t + y_{t+1}) \overset{i.i.d.}{\sim} N\left(0, 2\sigma^2\right), \quad t = 1, 2, ..., T-1, \tag{7}$$

which implies that $\mathbf{D}_2\mathbf{y}$ follows a Multivariate Normal distribution with

$$E(\mathbf{D}_2\mathbf{y}) = \mathbf{0}, \quad Var(\mathbf{D}_2\mathbf{y}) = E[(\mathbf{D}_2\mathbf{y})(\mathbf{D}_2\mathbf{y})^T] = \begin{bmatrix} 2\sigma^2 & & \\ & \ddots & \\ & & 2\sigma^2 \end{bmatrix}.$$

Consequently, the expected value of the estimated error in Equation (6) is

$$E(\mathbf{e}^{HP}) = 2\lambda(\mathbf{I}_{T+1} + 2\lambda\mathbf{D}_2^T\mathbf{D}_2)^{-1}\mathbf{D}_2^T E(\mathbf{D}_2\mathbf{y}) = \mathbf{0},$$

and since $(\mathbf{I}_{T+1} + 2\lambda\mathbf{D}_2^T\mathbf{D}_2)^{-1}$ is a symmetric matrix, the covariance matrix

$$Var(\mathbf{e}^{HP}) = 8\lambda^2\sigma^2(\mathbf{I}_{T+1} + 2\lambda\mathbf{D}_2^T\mathbf{D}_2)^{-1}\mathbf{D}_2^T\mathbf{D}_2(\mathbf{I}_{T+1} + 2\lambda\mathbf{D}_2^T\mathbf{D}_2)^{-1}. \tag{8}$$

Therefore, we have the following theorem.

Theorem 1. *Let Assumptions 1 and 2 hold. If there is no change point in the time series $\{y_t\}_{t=0}^T$, then*

$$e_t^{HP} = \left(y_t - \hat{x}_t^{HP}\right) \sim N\left(0, Var(\mathbf{e}^{HP})_{tt}\right), \tag{9}$$

where $Var(\mathbf{e}^{HP})_{tt}$ denotes the t-th diagonal element of the covariance matrix $Var(\mathbf{e}^{HP})$, as defined in Eq. (8)*.*

In practice, inspired by Wahlberg et al. (2011), σ^2 can be estimated by

$$\hat{\sigma}^2 = \frac{1}{2(T-1)}\sum_{t=1}^{T-1}(y_{t-1} - 2y_t + y_{t+1})^2. \tag{10}$$

With Theorem 1 and Eq. (10), we can construct a confidence interval to detect change points within the data. Furthermore, a normality test can be employed to assess whether the tuning parameter λ in Eq. (11) is appropriately chosen. In Section 5, we demonstrate the overall performance the HP-based change point detection.

The challenge with HP-based change point detection lies in its tendency to identify multiple points around the actual change points rather than a single accurate point. A potential solution is to assume that the number of change points within a given time interval follows a Poisson process. This allows us to construct α-level confidence intervals for the true change points based on a given parameter λ in Eq. (4). To formalize this approach, we introduce the following assumption.

Assumption 3. *Let $\{y_t\}_{t=0}^T$ denote a sequence of random variables. Assume that the number of change points, $n(t)$, within a time interval of length t follows a Poisson process with rate parameter μ, such that*

$$p[n(t)] = \frac{(\mu t)^n}{n!} e^{-\mu t}, n(t) = 0, 1, 2, ...,$$

where $t > 0$ is the time interval.

Under Assumption 3, and utilizing the memoryless property of the exponential distribution, we can compute the probability of observing at least one change point in a given time segment. This leads to the following proposition.

Proposition 1. *Let Assumptions 1, 2, and 3 hold. Let T_{ind} denote the index of the time series $\{y_t\}_{t=0}^T$. Then, the probability of containing at least one change point in the time segment $[t, t+h]$ is given by*

$$P(T_{ind} < h) = 1 - (\mu h)e^{-\mu h},$$

where μ is the rate parameter of the Poisson process.

This proposition can be justified using two criteria. First, the memoryless property of the exponential distribution states that

$$P(T_{ind} < t + h | T_{ind} > t) = P(T_{ind} < h).$$

Second, by the definition of the Poisson process, the probability of observing at least one change point during the next h time points is given by

$$p[n(h) \geq 1] = 1 - (\mu h)e^{-\mu h}.$$

In practice, since the collected data is a time series with a discrete time index, we set $h = 1$ and estimate the rate parameter μ by computing the ratio of the total number of change points detected by the HP-based change point detection method to the length of the time series, $T + 1$.

Although Assumption 3 enables the construction of time intervals and confidence intervals, focusing on a single estimated change point with a confidence interval around it is often more desirable. To address this, we introduce the l_1-based change point detection.

2.3 l_1-based change point detection

Similar to HP-based change point detection, l_1 filtering also imposes a Lagrange penalty on the LSE. However, unlike HP filtering, l_1 filtering utilizes the l_1 norm as the penalty function. The loss function of the l_1 based change point detection is defined as

$$l_{l_1}(\hat{\mathbf{x}}) = (1/2)\|\mathbf{y} - \hat{\mathbf{x}}\|_2^2 + 2\lambda\|\mathbf{D}_2\hat{\mathbf{x}}\|_1, \tag{11}$$

where $\|\mathbf{u}\|_1 = \sum |u_t|$. Therefore, the solution of the loss function is

$$\hat{\mathbf{x}}^{l_1} = \underset{\hat{\mathbf{x}} \in \mathbb{R}^{T+1}}{\operatorname{argmin}} \left\{ (1/2)\|\mathbf{y} - \hat{\mathbf{x}}\|_2^2 + 2\lambda\|\mathbf{D}_2\hat{\mathbf{x}}\|_1 \right\}. \tag{12}$$

By the Lagrangian duality, solving Eq. (11) is equivalent to solving the following optimization problem.

$$\begin{aligned} &\underset{\mathbf{x} \in \mathbb{R}^T}{\text{minimize}} \left\{ (1/2)\|\mathbf{y} - \mathbf{x}\|^2 \right\} \\ &\text{subject to } \|\mathbf{D}_2\mathbf{x}\|_1 \leq m, \end{aligned} \tag{13}$$

where $m > 0$ and the Lagrange multiplier λ in Eq. (1) is negatively correlated to the value of m. Hence, similar to the HP-based change point detection, we have the following assumption.

Assumption 4. *There exists a constant $m \in (0, \infty)$ such that the following smoothness condition holds for the expected sequence, $\{x_t\}_{t=0}^T$.*

$$\|\mathbf{D}_2\mathbf{x}\|_1 = \sum_{t=2}^{T} |x_{t-1} - 2x_t + x_{t+1}| \leq m.$$

Note that the Lagrange multiplier λ in Eq. (2) is negatively correlated to the value of m. Therefore, solving the problem under Assumptions 1 and 4 is equivalent to finding the LSE of Eq. (11).

Although the loss function of the l_1-based change point detection is convex, we cannot directly apply the gradient descent algorithm to update the parameters due to the non-differentiability of the l_1-norm at 0. We will further discuss optimization algorithms based on gradient descent in Section 4.

Let $\hat{\mathbf{x}}^{l_1}$ is the optimal value of Eq. (11). Then, the sub-gradient condition is satisfied as

$$\nabla l_{l_1}(\hat{\mathbf{x}}^{l_1}) = \hat{\mathbf{x}}^{l_1} - \mathbf{y} + 2\lambda \mathbf{D}_2^T sgn(\mathbf{D}_2 \hat{\mathbf{x}}^{l_1}) = 0, \tag{14}$$

where the sign function $sgn(x)$ is defined as

$$sgn(x) = \begin{cases} 1, & x > 0, \\ -1, & x < 0, \\ 0, & x = 0, \end{cases}$$

and $\nabla l_{l_1}(\hat{\mathbf{x}}^{l_1})$ represents the sub-gradient of Eq. (11). Inspired by Tibshirani (1996), since $sgn(x) \approx x/|x|$, Eq. (14) can be approximated by

$$\hat{\mathbf{e}}^{l_1} = (\mathbf{y} - \hat{\mathbf{x}}^{l_1}) \approx 2\lambda \mathbf{D}_2^T \mathbf{W}^{-1} \mathbf{D}_2 \hat{\mathbf{x}}^{l_1}, \tag{15}$$

where $\mathbf{W}$ is an $(T-1) \times (T-1)$ diagonal matrix with the diagonal elements

$$|\hat{x}_{t-1}^{l_1} - 2\hat{x}_t^{l_1} + \hat{x}_{t+1}^{l_1}|, \quad t = 1, 2, ...T-1,$$

leading to $\mathbf{W}^{-1}$ be an $(T-1) \times (T-1)$ diagonal matrix with the diagonal elements

$$\frac{1}{|(\mathbf{D}_2 \hat{\mathbf{x}}^{l_1})_t|} = \frac{1}{|\hat{x}_{t-1}^{l_1} - 2\hat{x}_t^{l_1} + \hat{x}_{t+1}^{l_1}|}, \quad t = 1, 2, ...T-1.$$

With Eq. (15), we can approximate the l_1-based estimate by a HP-based estimate format,

$$\tilde{\mathbf{x}}^{l_1} = (\mathbf{I}_{T+1} + 2\lambda \mathbf{D}_2^T \mathbf{W}^{-1} \mathbf{D}_2)^{-1} \mathbf{y},$$

where $\tilde{\mathbf{x}}^{l_1} \approx \hat{\mathbf{x}}^{l_1}$ is the approximation. Consequently, the approximation of the error term for the l_1-based estimate is

$$\tilde{\mathbf{e}}^{l_1} = (\mathbf{y} - \tilde{\mathbf{x}}^{l_1}) = 2\lambda (\mathbf{I}_{T+1} + 2\lambda \mathbf{D}_2^T \mathbf{W}^{-1} \mathbf{D}_2)^{-1} \mathbf{D}_2^T \mathbf{W}^{-1} \mathbf{D}_2 \mathbf{y}.$$

Given the Assumption 1 and 4 and assuming there is no change point in the data, the conditional expected value of error become

$$E(\tilde{\mathbf{e}}^{l_1} | \hat{\mathbf{x}}^{l_1}) = 2\lambda (\mathbf{I}_{T+1} + 2\lambda \mathbf{D}_2^T \mathbf{W}^{-1} \mathbf{D}_2)^{-1} \mathbf{D}_2^T \mathbf{W}^{-1} E(\mathbf{D}_2 \mathbf{y}) = \mathbf{0}.$$

This implies that $E(\hat{\mathbf{x}}^{l_1}) \approx E(\tilde{\mathbf{x}}^{l1}) = E(\mathbf{y})$, making it an unbiased estimator.

However, similar to the LASSO estimators, one significant challenge lies in accurately estimating the variance of the error term, $Var(\hat{\mathbf{e}}^{l_1} | \hat{\mathbf{x}}^{l_1})$. One potential approach to address this challenge is to employ Cross-Validation-based variance estimation, which can enhance the robustness and reliability of variance estimation (Reid et al., 2016).

In our numerical experiments, $Var(\hat{\mathbf{e}}^{l_1} | \hat{\mathbf{x}}^{l_1})$ is observed to closely approximate the error variance σ^2. Based on the bias-variance tradeoff formula (Hastie, 2009), the conditional covariance matrix for the error term is diagonal, and its diagonal elements are given by

$$Var(\hat{\mathbf{e}}^{l_1} | \hat{\mathbf{x}}^{l_1}) = E[(\mathbf{y} - \hat{\mathbf{x}}^{l_1})(\mathbf{y} - \hat{\mathbf{x}}^{l_1})^T | \hat{\mathbf{x}}^{l_1}] = \sigma^2 + Var(\hat{\mathbf{x}}^{l_1}) + \left(Bias[(\hat{\mathbf{x}}^{l_1})_t]\right)^2 = \sigma^2 + Var(\hat{\mathbf{x}}^{l_1}).$$

This result implies that $Var(\hat{\mathbf{x}}^{l_1}) \approx 0$.

Now, revisit Eq. (11) and consider the LSE for the loss function as a Maximum Likelihood Estimate (MLE) by taking the negative log on both side.

$$\begin{aligned} \log lik_{l_1}(\hat{\mathbf{x}}) &= -(1/2)\|\mathbf{y} - \hat{\mathbf{x}}\|_2^2 - 2\lambda \|\mathbf{D}_2 \hat{\mathbf{x}}\|_1 \\ &= \prod_{t=0}^{T} \exp\left\{ -\frac{1}{2}(y_t - \hat{x}_t)^2 \right\} \prod_{t=1}^{T-1} \exp\left\{ -\frac{|\hat{x}_{t-1} - 2\hat{x}_t + \hat{x}_{t+1}|}{1/(2\lambda)} \right\}, \end{aligned} \tag{16}$$

where $lik_{l_1}(\hat{\mathbf{x}})$ is the log-likelihood function. Consequently, by the Assumptions 1 and 4, and if there is no change point, we have the following theorem.

Theorem 2. *Let Assumptions 1 and 4 hold, and let $\hat{\mathbf{x}}^{l_1}$ be the solution of Eq.* (11)*. If the time series $\mathbf{y}$ contains no change points, then the elements of $\mathbf{D}_2\hat{\mathbf{x}}^{l_1}$ are i.i.d. following a Laplace distribution (or double exponential distribution) with a location parameter 0 and a scale parameter $1/(2\lambda)$. That is,*

$$\left(\mathbf{D}_2\hat{\mathbf{x}}^{l_1}\right)_t = (\hat{x}^{l_1}_{t-1} - 2\hat{x}^{l_1}_t + \hat{x}^{l_1}_{t+1}) \overset{i.i.d.}{\sim} Laplace(0, 1/(2\lambda)),$$

for $t = 1, 2, ..., T-1$. The probability density function is given by

$$f(\hat{x}^{l_1}_{t-1} - 2\hat{x}^{l_1}_t + \hat{x}^{l_1}_{t+1}) = \frac{1}{1/\lambda}\exp\left\{-\frac{|\hat{x}^{l_1}_{t-1} - 2\hat{x}^{l_1}_t + \hat{x}^{l_1}_{t+1}|}{1/(2\lambda)}\right\}.$$

Additionally, the variance of $\left(\mathbf{D}_2\hat{\mathbf{x}}^{l_1}\right)_t$ is

$$\frac{1}{2\lambda^2} = Var\left[\left(\mathbf{D}\hat{\mathbf{x}}^{l_1}\right)_t\right].$$

Note that since $\hat{\mathbf{x}}^{l_1}$ is the minimum solution for Eq. (12), we have

$$(1/2)\|\mathbf{y} - \hat{\mathbf{x}}^{l_1}\|_2^2 + 2\lambda\|\mathbf{D}_2\hat{\mathbf{x}}^{l_1}\|_1 \leq 2\lambda\|\mathbf{D}_2\mathbf{y}\|_1.$$

Since $(1/2)\|\mathbf{y} - \hat{\mathbf{x}}^{l_1}\|_2^2 \geq 0$, by the Cauchy-Schwarz inequality, we have

$$\|\mathbf{D}_2\hat{\mathbf{x}}^{l_1}\|_1 \leq \|\mathbf{D}_2\mathbf{y}\|_1 \leq \sqrt{T-1}\|\mathbf{D}_2\mathbf{y}\|_2, \tag{17}$$

This implies

$$\sum_{t=1}^{T-1}\left[(\mathbf{D}_2\hat{\mathbf{x}}^{l_1})_t\right]^2 = \|\mathbf{D}_2\hat{\mathbf{x}}^{l_1}\|_2^2 \leq \|\mathbf{D}_2\hat{\mathbf{x}}^{l_1}\|_1^2 \leq (T-1)\|\mathbf{D}_2\mathbf{y}\|_2^2. \tag{18}$$

Assuming there is no change point in the data, by taking the expected value for both sides of Eq. (18), we obtain

$$\sum_{t=1}^{T-1} E\left(\left[(\mathbf{D}_2\hat{\mathbf{x}}^{l_1})_t\right]^2\right) \leq 2(T-1)^2\sigma^2,$$

which leads to

$$E\left(\left[(\mathbf{D}_2\hat{\mathbf{x}}^{l_1})_t\right]^2\right) = Var\left[\left(\mathbf{D}\hat{\mathbf{x}}^{l_1}\right)_t\right] \leq 2(T-1)\sigma^2, \quad t = 1, 2, ..., T-1.$$

With Theorem 2, we have the following proposition.

Proposition 2. *Let Assumptions 1 and 4 hold. If there are no change points in the data, the parameter λ in Eq.* (11) *has a lower bound*

$$\frac{1}{(T-1)\sigma} \leq \lambda. \tag{19}$$

In addition, under Assumption 1, by employing the classical variance estimator, $(1/T)\sum_{t=0}^{T}\left(y_t - \hat{x}^{l_1}_t\right)^2$ to approximate the variance of error term, we have the following theorem.

Theorem 3. *Let Assumptions 1 and 4 hold. Under these conditions, and let $\hat{\mathbf{x}}^{l_1}$ be the solution of Eq.* (11)*, the estimated error terms $\{\hat{e}^{l_1}_t\}_{t=0}^T = \{y_t - \hat{x}^{l_1}_t\}_{t=0}^T$ are independent and identically distributed (i.i.d.) and follow a standard normal distribution, that is,*

$$\frac{\hat{e}^{l_1}_t}{\sqrt{\frac{1}{T}\sum_{t=0}^{T}\left(\hat{e}^{l_1}_t\right)^2}} = \frac{y_t - \hat{x}^{l_1}_t}{\sqrt{\frac{1}{T}\sum_{t=0}^{T}\left(y_t - \hat{x}^{l_1}_t\right)^2}} \overset{i.i.d.}{\sim} N(0,1),$$

where $t = 0, 1, 2, ..., T$.

Furthermore, similar to the property of the lasso estimator, if there is no change point in the data and the penalty parameter λ is sufficiently large such that $E(\mathbf{D}\hat{\mathbf{x}}^{l_1}) = \mathbf{0}$, then based on the bias-variance tradeoff formula and Theorem 2, the variance of $\mathbf{D}_2\hat{\mathbf{e}}^{l_1}$ is given by

$$Var(\mathbf{D}_2\hat{\mathbf{e}}^{l_1}) = E[(\mathbf{D}_2\hat{\mathbf{e}}^{l_1})(\mathbf{D}_2\hat{\mathbf{e}}^{l_1})^T] = 2\sigma^2 + Var(\mathbf{D}_2\hat{\mathbf{x}}^{l_1}) = \left(2\sigma^2 + \frac{1}{2\lambda}\right)\mathbf{I}_{T-1} \approx 2\sigma^2\mathbf{I}_{T-1},$$

where $\mathbf{I}_{T-1} \in \mathbb{R}^{(T-1)\times(T-1)}$ is the identity matrix.

Another advantage of l_1-filtering is that, by the definition of degree of freedom in the LASSO parameter, which is the number of effective parameters (ZOU et al., 2007), we can also approximate the number of maximum change point in the time series by the degree of freedom, that is,

$$df(\lambda) = \frac{1}{2\sigma^2}\sum_{t=1}^{T-1} Cov[(\mathbf{D}_2\hat{\mathbf{x}})_t, (\mathbf{D}_2\mathbf{y})_t],$$

where $df(\lambda)$ represents the degree of freedom and provides an interpretation as the maximum number of change points. This leads to the following estimator

$$\hat{df}(\lambda) \approx tr[\mathbf{D}_2(\mathbf{I}_{T+1} + 2\lambda\mathbf{D}_2^T\mathbf{W}^{-1}\mathbf{D}_2)^{-1}], \tag{20}$$

where $tr(\cdot)$ is the trace of a matrix, and $\mathbf{W}^{-1} = diag(1/|\hat{x}^{l_1}_{t-1} - 2\hat{x}^{l_1}_t + \hat{x}^{l_1}_{t+1}|)$ be the $(T-1)\times(T-1)$ diagonal matrix.

Therefore, an efficient way to identify change points is by setting a threshold for $|(\mathbf{D}_2\hat{\mathbf{x}}^{l_1})_t|$. Inspired by Harchaoui and Lévy-Leduc (2010), the criterion for identifying change points is defined as

$$|(\mathbf{D}_2\hat{\mathbf{x}}^{l_1})_t| = |\hat{x}^{l_1}_{t-1} - 2\hat{x}^{l_1}_t + \hat{x}^{l_1}_{t+1}| \geq \text{threshold}. \tag{21}$$

Under this condition, the time t is considered a change point, where $t = 1, 2, ..., T-1$. The minimum threshold can be determined based on the estimated maximum number of change points, $\hat{df}(\lambda)$. Alternatively, the threshold can be set to the $(1-\alpha)\%$ percentile.

3 Shapiro-Wilk normality test to eliminate the range of λ

Using Theorem 1, we can eliminate certain values of λ when applying HP-based change point detection by performing hypothesis testing with the following formulation.

H_0: The error term is normally distribution, $\quad H_a$: The error term is not normally distribution.

As noted by Razali et al. (2011), the Shapiro-Wilk normality test (Shaphiro and Wilk, 1965) has the highest statistical power among commonly used methods for testing normality. The test statistic for this analysis is defined as

$$W = \frac{(\sum_{t=0}^{T} a_t \hat{e}^{HP}_{(t)})^2}{\sum_{t=0}^{T}\left(\hat{e}^{HP}_{(t)}\right)^2}, \tag{22}$$

where $\hat{e}^{HP}_{(0)} \leq \hat{e}^{HP}_{(1)} \leq \cdots \leq \hat{e}^{HP}_{(T)}$ are the ordered elements of the error vector $\hat{\mathbf{e}}^{HP}$, defined as $\hat{\mathbf{e}}^{HP} = \mathbf{y} - \hat{\mathbf{x}}^{HP}$. The vector $\mathbf{a} = \{a_t\}_{t=0}^{T}$ is given by

$$\mathbf{a} = \frac{\mathbf{m}^T Var(\hat{\mathbf{e}}^{HP})^{-1}}{\|\mathbf{m}^T Var(\hat{\mathbf{e}}^{HP})^{-1}\|_2},$$

where $\mathbf{m} = \{m_t\}_{t=0}^{T}$ represents the expected values of the order statistics of i.i.d. random variables drawn from the standard normal distribution, and $Var(\hat{\mathbf{e}}^{HP}$ can be estimated by Eq. (8) and Eq. (10).

The value of W lies between 0 and 1. If W is close to 0, it leads to the rejection of the null hypothesis, indicating that the error term does not follow a normal distribution. Consequently, the corresponding value of λ should be eliminated. However, in our numerical experiments, this method is not effective for the HP-based change point detection. This is because $\|\mathbf{D}_2\mathbf{x}\|_2^2$ in Eq. (4) implies that the prior of $\mathbf{D}_2\mathbf{x}$ follows a normal distribution. As a result, the p-values for the normality test are very large, failing to reject the null hypothesis.

In contrast, this normality test is very effective in the case of l_1-based change point detection. To eliminate certain values of λ when applying l_1-based change point detection using Theorem 3, we replace $\hat{\mathbf{e}}^{HP}_t$ with

$$\frac{\hat{e}^{l_1}_t}{\sqrt{\frac{1}{T}\sum_{t=0}^{T}\left(\hat{e}^{l_1}_t\right)^2}},$$

where $\hat{e}^{l_1}_t = y_t - \hat{x}^{l_1}$. This leads to

$$Var\left(\frac{\hat{e}^{l_1}_t}{\sqrt{\frac{1}{T}\sum_{t=0}^{T}\left(\hat{e}^{l_1}_t\right)^2}}\right) = \mathbf{I}_{T+1},$$

where $\mathbf{I}_{T+1} \in \mathbb{R}^{(T+1)\times(T+1)}$ is the identity matrix. Similar to the hypothesis testing for HP-based change point detection, we should eliminate the value of λ in Eq. (11) if the Shapiro-Wilk statistic W is close to zero, indicating that the error terms deviate significantly from the Normal distribution assumption. In our numerical experiments, this method proves particularly effective in eliminating large values of λ.

Furthermore, the lower bound of λ can be derived from Eq. (19), where σ^2 is estimated by setting an extremely large λ and computing the mean squared error (MSE) of the model as

$$\hat{\sigma}^2 = \frac{1}{T}\sum_{t=0}^{T}\left(\hat{e}_t^{l_1}\right)^2.$$

4 Optimization method for l_1-based change point detection

Another key challenge in $l_1$based change point detection lies in the optimization method. A common approach is gradient descent, which assumes the objective function $f(x)$ is convex and differentiable, The gradient update for x is defined by

$$x^{(i+1)} = x^{(i)} - s^{(i)}\nabla f(x^{(i)}), \tag{23}$$

where $\nabla f(x^{(i)})$ represents the gradient of f at iteration i, and $s^{(i)}$ is the step size for the ith update. However, the penalty term in (11) includes the absolute value function, which is non-differentiable but sub-differentiable. To overcome this issue, a classical and effective method is proximal gradient descent (Hastie et al., 2015; Liu et al., 2020b), which extends gradient-based techniques to handle non-differentiable terms.

4.1 Proximal gradient descent

Proximal gradient descent applies classical gradient descent to the differentiable part of the loss function and subsequently projects the solution onto the constrained space, corresponding to the non-differentiable part of the loss function, using the proximal operator. This approach results in a generalized gradient update rule (Hastie et al., 2015).

Algorithm 1: Proximal gradient descent

Input:

Observed data $\mathbf{y}$, tuning parameter $\lambda > 0$, step size $s > 0$, maximum number of iterations $I > 0$.

Set the initial guess $\mathbf{x}^{(0)} \in \mathbb{R}^{(T+1)}$;
Set $i = 0$;
while $i \leq I$ **do**
  Gradient step
    $\mathbf{x_{temp}} = \mathbf{x}^{(i)} - s(\mathbf{x}^{(i)} - \mathbf{y})$;
    $\mathbf{z} = \mathbf{D}_2\mathbf{x_{temp}}$;
  Proximal update
    $(\mathbf{D}\mathbf{x}^{(i+1)})_t = sign(z_t^{(i)})(|z_t^{(i)}| - \lambda s^{(i)})_+$;
  Update $\mathbf{x}$
    $x_0^{(i+1)} = y_0$;
    $x_T^{(i+1)} = y_T$;
    Compute the rest of the solution for $\mathbf{x}^{(i+1)}$ using $\mathbf{D}\mathbf{x}^{(i+1)}$;
  Increment $i \leftarrow i + 1$;
end

In the context of Eq. (11), and given that $\|\mathbf{D}_2\mathbf{x}\|_2^2 \leq 16\|\mathbf{x}\|_2^2$, the generalized gradient update is defined as

$$\mathbf{x}^{(i+1)} = \underset{\mathbf{x}\in\mathbb{R}^{T+1}}{\operatorname{argmin}}\left\{(1/2)\|\mathbf{y} - \mathbf{x}^{(i)}\|_2^2 + (\mathbf{x}^{(i)} - \mathbf{y})^T(\mathbf{x} - \mathbf{x}^{(i)}) + \frac{1}{2s^{(i)}}\|\mathbf{D}_2\mathbf{x} - \mathbf{D}_2\mathbf{x}^{(i)}\|_2^2 + 2\lambda\|\mathbf{D}_2\mathbf{x}\|_1\right\},$$

where i is the ith iteration and $s^{(i)}$ is the step size at the ith iteration. Under assumptions 1 and 4, the proximal operator can be defined as

$$\mathbf{prox}(\mathbf{z}^{(i)}) = \underset{\mathbf{D}_2\mathbf{x}\in\mathbb{R}^{T-1}}{\operatorname{argmin}}\left\{\frac{1}{2}\|\mathbf{D}_2\mathbf{x} - \mathbf{z}^{(i)}\|_2^2 + 2\lambda s^{(i)}\|\mathbf{D}_2\mathbf{x}\|_1\right\},$$

The solution to this minimization problem can be computed element-wise using the soft-thresholding operator, defined as

$$[\mathbf{S}(\mathbf{z}^{(i)})]_t = sign(z_t^{(i)})(|z_t^{(i)}| - \lambda s^{(i)})_+, \quad t = 1, 2, ..., T-1,$$

where $(x)_+ = \max\{x, 0\}$. This result in a proximal gradient descent algorithm (see Algorithm 1).

The main disadvantage of proximal gradient descent lies in determining the appropriate step size s. If the step size is too large, it may overshoot the optimal value, leading to divergence. Conversely, if the step size is too small, the algorithm will require an excessive number of iterations to converge to the optimal value, making it inefficient. A more effective optimization method for addressing this issue is the Resilient Backpropagation Algorithm (RPROP), as proposed by Riedmiller and Braun (1993).

4.2 Resilient Backpropagation Algorithm (RPROP)

In the l_1-based change point detection, the advantage of applying RPROP is that it relies solely on the sign of the gradient in Eq. (23) to adjust the step size and determine the direction of the update. This approach is particularly beneficial as it works directly with the sub-gradient of Eq. (11), making it well-suited for handling the non-differentiability of the l_1-norm.

Algorithm 2: Resilient Backpropagation Algorithm (RPROP)

Input:
Observed data $\mathbf{y}$, tuning parameter $\lambda > 0$, maximum number of iterations $I > 0$.

Set the increasing factor $\eta_+ = 1.2$;
Set the decreasing factor $\eta_- = 0.5$;
Set the step size upper limit $s_{max} = 50$;
Set the step size lower limit $s_{min} = 1e^{-6}$;
Let the initial guess $\mathbf{x}^{(1)} \in \mathbb{R}^{(T+1)}$;
Let the initial step size $s^{(0)} = 1e^{-2}$;
Let the initial sub-gradient $\nabla l_{l_1}(\mathbf{x}^{(0)}) = 0$;
for $i = 1$ *to* I **do**
    $\nabla l_{l_1}(\mathbf{x}^{(i)}) = \mathbf{x}^{(i)} - \mathbf{y} + 2\lambda \mathbf{D}_2^T sgn(\mathbf{D}_2 \mathbf{x}^{(i)})$;
    if $\nabla l_{l_1}(\mathbf{x}^{(i)})^T \nabla l_{l_1}(\mathbf{x}^{(i-1)}) > 0$ **then**
        $s^{(i)} = \min\left\{s^{(i-1)}\eta_+, s_{max}\right\}$;
    end
    else if $\nabla l_{l_1}(\mathbf{x}^{(i)})^T \nabla l_{l_1}(\mathbf{x}^{(i-1)}) < 0$ **then**
        $s^{(i)} = \max\left\{s^{(i-1)}\eta_-, s_{min}\right\}$;
        $\nabla l_{l_1}(\mathbf{x}^{(i)}) = 0$
    end
    else if $\nabla l_{l_1}(\mathbf{x}^{(i)})^T \nabla l_{l_1}(\mathbf{x}^{(i-1)}) = 0$ **then**
        $s^{(i)} = s^{(i-1)}$;
    end
    $\mathbf{x}^{(i+1)} = \mathbf{x}^{(i)} - s^{(i)} sign[\nabla l_{l_1}(\mathbf{x}^{(i)})]$;
end

Algorithm 2 demonstrates the implementation of RPROP for efficiently finding the optimal solution to Eq. (11). In the numerical experiments, RPROP successfully converges within 100 iterations.

5 Numerical illustration

We simulate a time series random variable, y_t, for $t = 0, 1, \ldots, 100$, under two scenarios: one without any change points and another with change points. Both the HP-based and l_1-based change point detection methods are applied and compared to the SSA change point detection method to evaluate their performance. Additionally, we calculate the Root Mean Squared Error (RMSE) for various values of the tuning parameter λ for both the HP-based and l_1-based methods.

The RMSE is defined as

$$RMSE = \sqrt{\frac{1}{T}\sum_{t=0}^{T}(y_t - \hat{x}_t)^2},$$

where $\hat{x}_t$ represents the estimated trend.

5.1 No change point scenario

In the scenario of no change point, we have

$$y_0 = \epsilon_0, \quad y_t = 5 + y_{t-1} + \epsilon_t, \quad t = 0, 1, ..., 99$$

where $\epsilon_t \overset{i.i.d.}{\sim} N(0, 5^2)$. We conduct this simulation 1000 times to compute the empirical accuracy rate (see Figure 1).

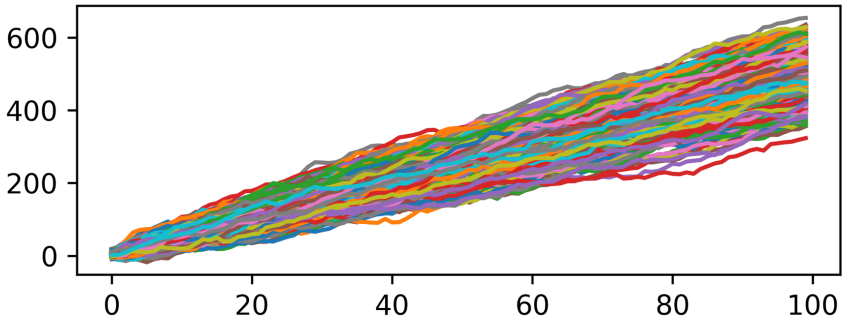

Figure 1: Plot of simulation data for 1,000 time series ($T = 99$), generated without any change points.

5.1.1 HP-based change point detection result

In the HP-based change point detection method, selecting the optimal value of the tuning parameter λ is crucial. However, relying on the Shapiro-Wilk normality test to narrow down the range of λ values for this method proves to be ineffective.

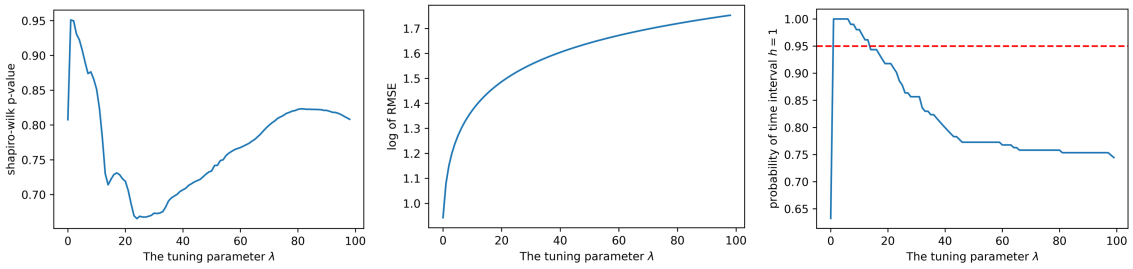

(a) (b) (c)

Figure 2: Range of λ: 1 to 100. (a) P-values from the Shapiro-Wilk normality test, (b) logarithm of the RMSE, and (c) probability of detecting at least one change point within a given time interval $[t, t + h]$ using the HP-based change point detection method.

Figure 2 presents a representative example from 1,000 simulated time series, using a grid search for λ values ranging from 1 to 100. Figure 2a shows the p-values from the Shapiro-Wilk normality test, all exceeding 0.05, indicating that none of the λ values lead to the rejection of the null hypothesis. Figure 2b displays the logarithm of the RMSE, revealing a clear trend of increasing error as λ becomes larger. These findings suggest that residual distribution testing is not effective for the HP-based change point detection method. Finally, Figure 2c illustrates the estimated probability of containing at least one change point within a given time interval $[t, t + 1]$, with the red dashed line marking the 95% threshold. Notably, the largest λ with a probability exceeding 95% occurs at $\lambda = 13$.

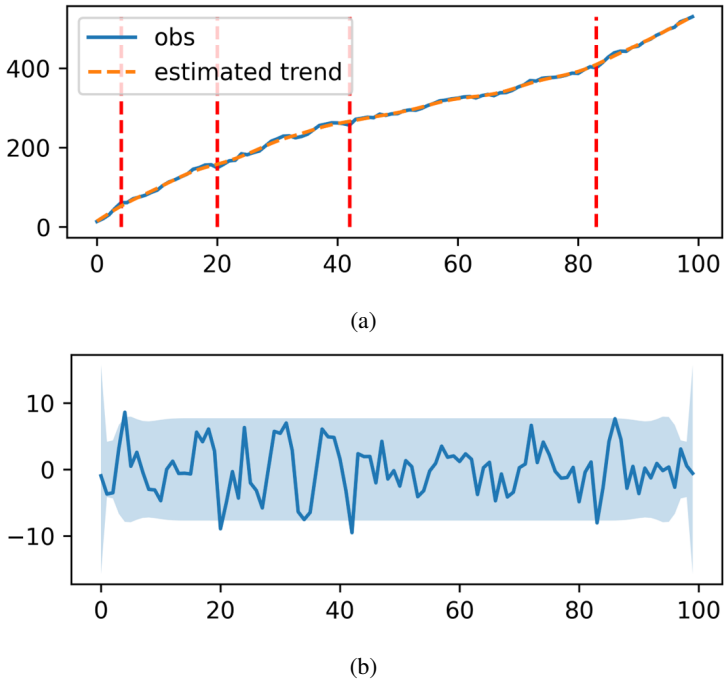

Figure 3: A representative result of the HP-based change point detection method. (a) The dashed line represents the HP trend filter, and the solid line represents the observed data. (b) The shaded area indicates the 95% Confidence Interval (CI) derived from Theorem 1.

The final result of the HP-based change point detection is presented in Figure 3. In this representative example, the HP-based method identifies change points in the time intervals 4-5, 20-21, 42-43, and 83-84 (see Figure 3a). However, since this simulated data contains no actual change points, these detections are false positives. Figure 3b illustrates the error term based on Eq. (6), with the shaded area representing the 95% CI. The variance is computed using Eq. (8).

5.1.2 l_1-based change point detection result

In the l_1-based change point detection method, the Shapiro-Wilk normality test become very effective to selecting optimal value of the tuning parameter λ.

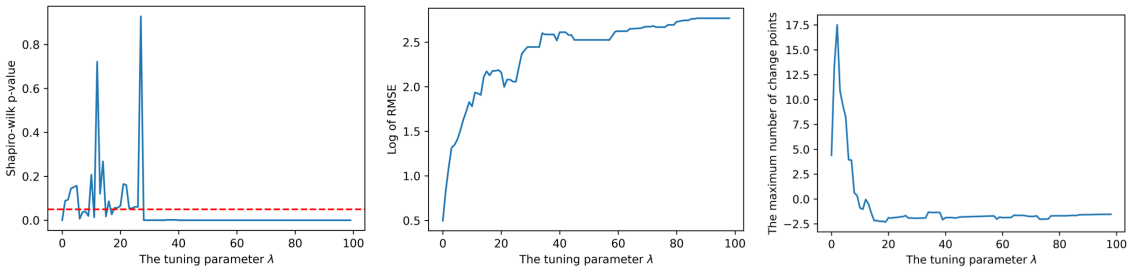

Figure 4: Range of λ: 1 to 100. (a) P-values from the Shapiro-Wilk normality test, (b) logarithm of the RMSE, and (c) estimated maximum number of change points based on the degrees of freedom derived from the l_1-based change point detection method (Eq. (20)).

Figure 4 displays a representative example from 1,000 simulated time series, with a grid search conducted for λ values ranging from 1 to 100. Figure 4a shows the p-values from the Shapiro-Wilk normality test, with the red dashed line indicating the significance level of 0.05. The smallest λ value with a p-value exceeding 0.05 is $\lambda = 1$, with a p-value

of approximately 0.0883. Additionally, when λ becomes too large, the p-value consistently falls below 0.05; in this example, this occurs when $\lambda \geq 23$. Similar to the HP filter, the RMSE increases as λ grows, as illustrated in Figure 4b.

A key advantage of the proposed l_1-based change point detection method is its ability to use the estimated degrees of freedom to determine the maximum number of change points and automatically calculate the threshold in Eq. (21). Figure 4c presents the maximum number of change points identified for different λ values. When $\lambda = 0$, the method identifies 98 change points, suggesting that nearly every observed point is considered a change point. However, when $\lambda = 1$, the maximum number of change points for this example is reduced to 4.

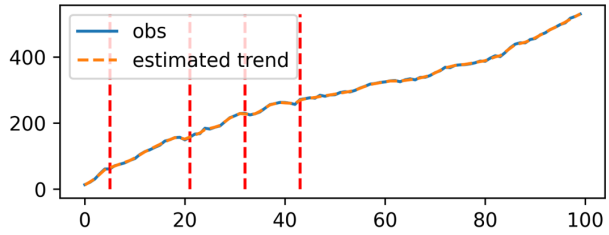

(a)

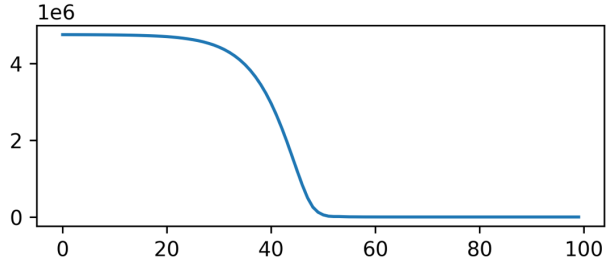

(b)

Figure 5: A representative result of the l_1-based change point detection method. (a) The dashed line represents the l_1 trend filter, and the solid line represents the observed data. (b) The RPROP optimization process of the loss function.

The results of the l_1-based change point detection are presented in Figure 5. In this representative example, the method identifies change points at time intervals 5-6, 21-22, 32-33, and 43-44 (see Figure 5a). However, as the simulated data contains no actual change points, these detections are false positives. Figure 5b illustrates the iteration steps of the RPROP algorithm, where the loss function reaches its minimum after approximately 50 iterations. The results stabilize around 100 iterations.

5.1.3 Model comparisons

We compared our proposed method with the PELT method using the l_2 model, with the penalty parameter set to 1. Figure 6 presents a representative example of the PELT method, where 19 change points were detected—all of which are false positives.

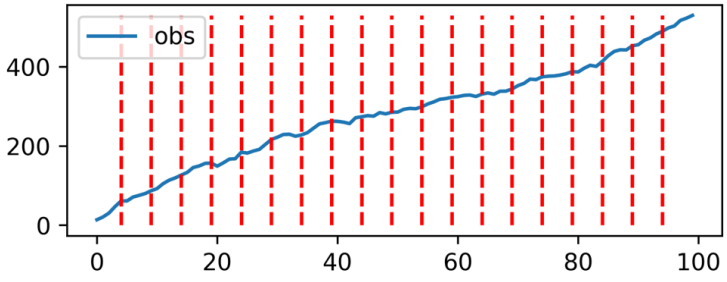

Figure 6: A representative result of the PELT method.

Table 1: Number of change points detected across 1,000 simulated time series in the no change point scenario.

Method	mean	std	min	25%	50%	75%	max
PELT	18.841	0.405	16	19	19	19	19
HP	4.284	3.379	0	2	4	6	26
l_1	5.681	2.699	0	4	6	7	14

As shown in Table 1, the PELT method demonstrated strong consistency across 1,000 simulations. On average, the PELT method detected 19 change points, resulting in the highest false positive rate. In contrast, the HP filter identified an average of 4 change points, achieving the lowest false positive rate. For the l_1-based method, we set the threshold based on the maximum number of change points, representing the most conservative threshold. Consequently, compared to the HP-based method, it exhibited slightly higher false positive rates. However, in practice, selecting a smaller threshold for the l_1-based method could significantly improve its performance.

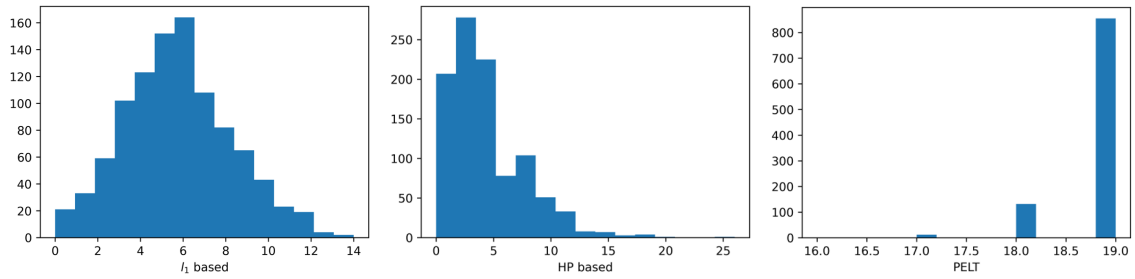

(a) (b) (c)

Figure 7: Histograms showing the number of change points detected across 1,000 simulated time series under the no change point scenario: (a) l_1-based change point detection method, (b) HP-based change point detection method, and (c) PELT method.

Figure 7 illustrates the empirical distribution of detected change points for all three methods. Among them, the PELT method exhibited the highest consistency across 1,000 simulations, followed by the l_1-based method.

5.2 Two change point scenario

In the scenario of two change point, we have

$$y_0 = \epsilon_0, \quad y_t = \begin{cases} 5 + y_{t-1} + \epsilon_t, & t = 0, 1, ..., 20 \\ -5 + y_{t-1} + \epsilon_t, & t = 21, ..., 50 \\ 5 + y_{t-1} + \epsilon_t, & t = 51, ..., 100 \end{cases}$$

where $\epsilon_t \overset{i.i.d.}{\sim} N(0, 5^2)$. This setting implies the data contains $K = 3$ segments (or 2 change points: $t = 20, 50$). We conduct this simulation 1000 times to compute the empirical accuracy rate.

5.2.1 HP-based change point detection result

Compared to the no-change-point scenario, the pattern of varying λ values for the HP-based change point detection method remains unchanged in the two change point scenario (see Figure 8). We select $\lambda = 13$ as it is the largest value with a probability exceeding 95% (see Figure 8c).

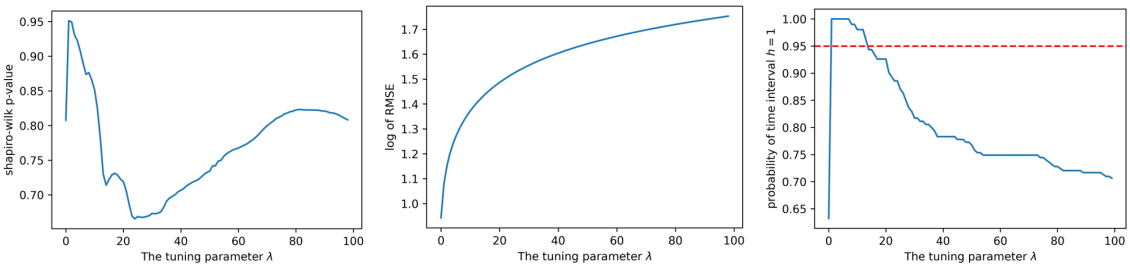

(a) (b) (c)

Figure 8: Range of λ: 1 to 100. (a) P-values from the Shapiro-Wilk normality test, (b) logarithm of the RMSE, and (c) probability of detecting at least one change point within a given time interval $[t, t+h]$ using the HP-based change point detection method.

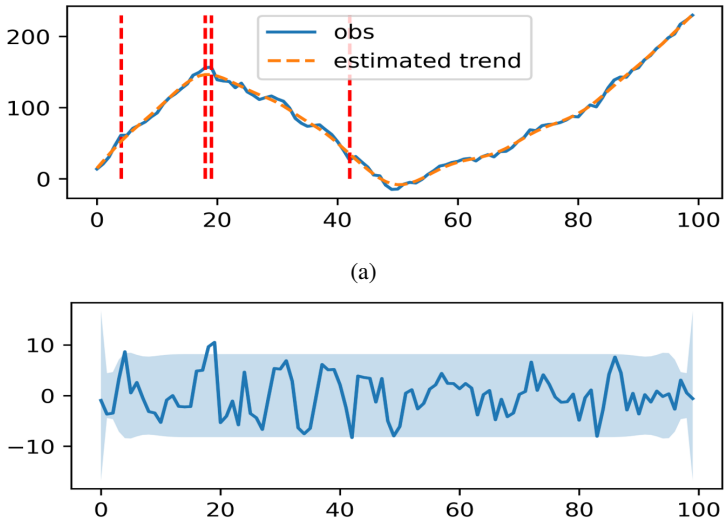

(a)

(b)

Figure 9: A representative result of the HP-based change point detection method. (a) The dashed line represents the HP trend filter, and the solid line represents the observed data. (b) The shaded area indicates the 95% Confidence Interval (CI) derived from Theorem 1.

The results of the HP-based change point detection are shown in Figure 9. In this representative example, the HP-based method identifies change points in the time intervals 4–5, 18–20, and 42–44 (see Figure 9a). Since the true change point is at 20, the false discovery rate is 2/3. Figure 9b depicts the error term calculated using Eq. (6), with the shaded area indicating the 95% confidence interval. The variance is determined using Eq. (8).

5.2.2 l_1-based change point detection result

Similar to the no-change-point scenario, the Shapiro-Wilk normality test is highly effective in selecting the optimal tuning parameter λ for the l_1-based change point detection method in the two-change-point scenario (see Figure 10). As shown in Figure 10a, $\lambda = 2$ is selected as the optimal value. Additionally, as indicated in Figure 10c, the maximum number of change points when $\lambda = 2$ is 15.

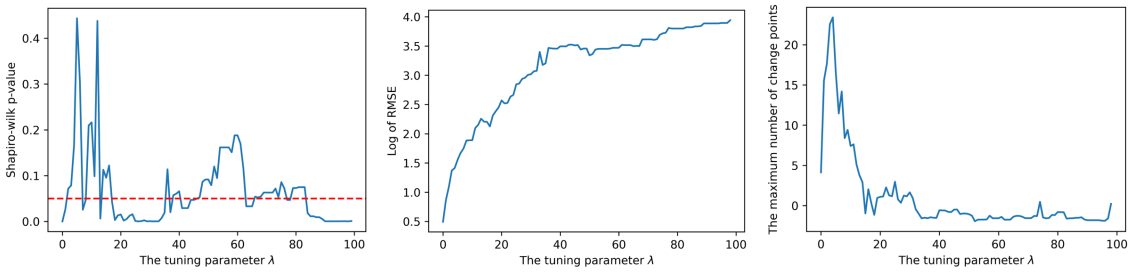

(a) (b) (c)

Figure 10: Range of λ: 1 to 100. (a) P-values from the Shapiro-Wilk normality test, (b) logarithm of the RMSE, and (c) estimated maximum number of change points based on the degrees of freedom derived from the l_1-based change point detection method (Eq. (20)).

The next step for the l_1-based change point detection method is to determine the appropriate threshold for Eq. (21). Figure 11 illustrates the change point results for various thresholds. When using the maximum number of detected change points in this example, 15 change points are identified. By merging adjacent change points into intervals, the resulting time intervals are: 5–6, 19–22, 25–26, 28–29, 31–32, 35–36, 39–41, 43–45, 50–51, 84–85, and 86–87 (see Figure 11a).

Alternatively, if the threshold is set to detect only five change points (i.e., using the 95% percentile of $|(\mathbf{D}_2\hat{\mathbf{x}}^{l_1})_t|$ in Eq. (21) as the threshold), and adjacent change points are merged, the resulting intervals are: 19–20, 28–29, 35–36, 43–44, and 50–51 (see Figure 11b). Finally, when the threshold is set to detect two change points, the resulting intervals are 19–20 and 50–51, which provide the most accurate results (see Figure 11c).

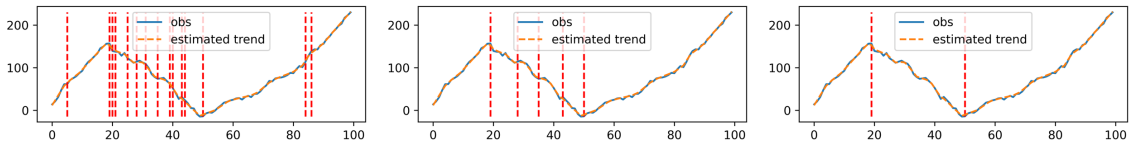

(a) (b) (c)

Figure 11: Representative results of the l_1-based change point detection method under varying thresholds: (a) Threshold set to detect up to 15 change points (maximum), (b) Threshold set to detect 5 change points (i.e., 95% percentile), and (c) Threshold set to detect 2 change points.

Table 2 shows the total number of true positive change points detected by the l_1-based change point detection method across all 1,000 simulations, using three different threshold settings: the maximum number of change points, the 95% percentile, and the threshold for detecting two change points. Table 2 also displays the average False Discovery Rate (FDR) across all 1,000 simulations, where

$$FDR = \frac{\text{False Positive}}{\text{False Positive} + \text{True Positive}},$$

indicating that a smaller FDR is preferred.

Table 2: The number of true positive change points detected by the l_1-based change point detection method

l_1-based true positive	Maximum number of change points	95% percentile (5)	2 change points
Change Point 20	718	604	420
Change Point 50	748	641	443
Average FDR	0.80	0.72	0.56

5.2.3 Model comparisons

We compared our proposed method with the PELT method using the l_2 model, with the penalty parameter set to 1. Figure 12 presents a representative example of the PELT method, where 19 change points were detected.

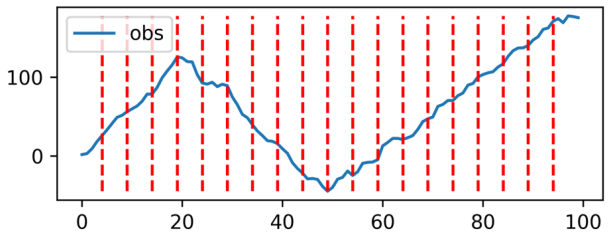

Figure 12: A representative result of the PELT method.

Table 3: The number of true positive change points detected by all three change point detection methods

True Positive	PELT	HP	l_1 (95% percentile)
Change Point 20	581	485	604
Change Point 50	597	490	641
Average FDR	0.94	0.72	0.72

Table 3 displays the overall performance of all three change point detection methods in the two change point scenario. In this scenario, the l_1-based change point detection method demonstrates the best performance, accurately detecting the most change points across all 1,000 samples while also achieving the smallest FDR. On the other hand, the PELT method detects the most change points but also exhibits the largest FDR, as it is most efficient in stationary situations.

The HP-based change point detection method shows the second-best performance in this scenario. Compared to the different settings of the l_1-based method (see Table 2), the HP-based method detects more change points than the l_1-based method when the threshold is set to detect two change points, although it has a larger FDR.

6 Real world data analysis

6.1 SNP500 index

We demonstrate the proposed method using daily data from the S&P 500 (SNP), collected from Yahoo Finance. The dataset spans January 27, 2020, to January 25, 2024, and we utilize the adjusted closing prices for demonstration purposes.

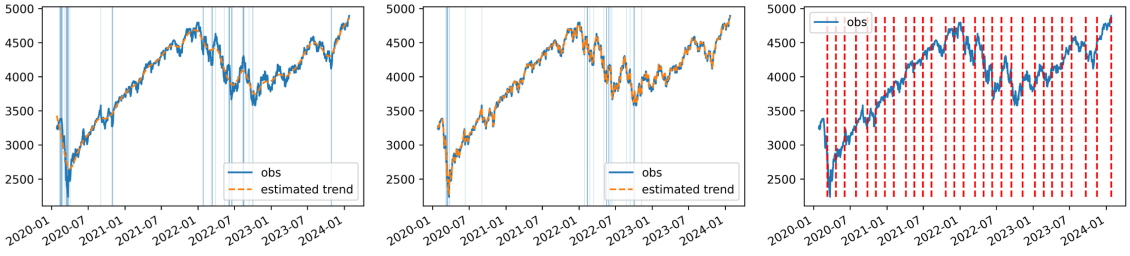

(a) (b) (c)

Figure 13: S&P 500 adjusted closing prices from January 27, 2020, to January 25, 2024, with a comparison of change point detection methods: (a) HP-based method: blue-shaded vertical regions indicate time intervals containing at least one change point. (b) l_1-based method: blue-shaded vertical regions indicate time intervals containing at least one change point. (c) PELT method: dashed vertical lines denote the detected change points.

Figure 13 illustrates the results of all three methods. Since stock market data is typically assumed to follow a random walk, the PELT method is unsuitable for this type of data (see Figure 13c). We applied the l_1-based method with $\lambda = 18$ and the Rprop algorithm with 400 iterations (see Figure 13b), which detected 19 time intervals as change points, including March 4–5, 2020, when COVID-19 began to significantly impact financial markets (Liu et al., 2020a;

Mazur et al., 2021); the period from March 9–18, 2020, which encompassed events such as "Black Monday I," "Black Thursday," and "Black Monday II," when U.S. stock markets experienced another major crash (Mazur et al., 2021); and February 23–24, 2022, when Russia invaded Ukraine (Astrov et al., 2022).

In comparison, the HP-based method with $\lambda = 7165$ detected 17 change points (see Figure 13a), 8 of which overlapped with those identified by the l_1-based method, including March 12–26, 2020, which covers "Black Thursday" and "Black Monday II." However, unlike the l_1-based method, the HP-based method failed to detect the February 23–24, 2022, change point associated with Russia's invasion of Ukraine. It did, however, successfully detect the period from October 26–30, 2023, marking the end of the United Auto Workers (UAW) strike (Rua and Tito, 2024).

7 Data availability statement

The data and the Python program that support the finding of this study are openly available at https://github.com/gdsdlxy/ChangePointDetection.git

8 Supporting information

Additional Supporting Information may be found online via https://github.com/gdsdlxy/ChangePointDetection.git

References

Alanqary, A., Alomar, A., and Shah, D. (2021). Change point detection via multivariate singular spectrum analysis. *Advances in Neural Information Processing Systems*, 34:23218–23230.

Astrov, V., Ghodsi, M., Grieveson, R., Holzner, M., Kochnev, A., Landesmann, M., Pindyuk, O., Stehrer, R., Tverdostup, M., and Bykova, A. (2022). Russia's invasion of ukraine: assessment of the humanitarian, economic, and financial impact in the short and medium term. *International Economics and Economic Policy*, 19(2):331–381.

Broomhead, D., Jones, R., and King, G. P. (1987). Topological dimension and local coordinates from time series data. *Journal of Physics A: Mathematical and General*, 20(9):L563.

Broomhead, D. S. and King, G. P. (1986). Extracting qualitative dynamics from experimental data. *Physica D: Nonlinear Phenomena*, 20(2-3):217–236.

Chan, K. W. and Yau, C. Y. (2017). High-order corrected estimator of asymptotic variance with optimal bandwidth. *Scandinavian Journal of Statistics*, 44(4):866–898.

Chen, J., Gupta, A. K., and Gupta, A. (2000). *Parametric statistical change point analysis*, volume 192. Springer.

Cho, H. and Fryzlewicz, P. (2024). Multiple change point detection under serial dependence: Wild contrast maximisation and gappy schwarz algorithm. *Journal of Time Series Analysis*, 45(3):479–494.

Csörgö, M. and Horváth, L. (1997). *Limit theorems in change-point analysis*. Wiley.

De Jong, R. M. and Sakarya, N. (2016). The econometrics of the hodrick-prescott filter. *Review of Economics and Statistics*, 98(2):310–317.

Golestan, S., Ramezani, M., Guerrero, J. M., Freijedo, F. D., and Monfared, M. (2013). Moving average filter based phase-locked loops: Performance analysis and design guidelines. *IEEE Transactions on Power Electronics*, 29(6):2750–2763.

Hamilton, J. D. (2018). Why you should never use the hodrick-prescott filter. *Review of Economics and Statistics*, 100(5):831–843.

Harchaoui, Z. and Lévy-Leduc, C. (2010). Multiple change-point estimation with a total variation penalty. *Journal of the American Statistical Association*, 105(492):1480–1493.

Hastie, T. (2009). The elements of statistical learning: data mining, inference, and prediction.

Hastie, T., Tibshirani, R., and Wainwright, M. (2015). Statistical learning with sparsity. *Monographs on statistics and applied probability*, 143(143):8.

Killick, R., Fearnhead, P., and Eckley, I. A. (2012). Optimal detection of changepoints with a linear computational cost. *Journal of the American Statistical Association*, 107(500):1590–1598.

Kim, J., Oh, H.-S., and Cho, H. (2024). Moving sum procedure for change point detection under piecewise linearity. *Technometrics*, pages 1–10.

Kim, S.-J., Koh, K., Boyd, S., and Gorinevsky, D. (2009). \ell_1 trend filtering. *SIAM review*, 51(2):339–360.

Li, L., Su, X., Zhang, Y., Lin, Y., and Li, Z. (2015). Trend modeling for traffic time series analysis: An integrated study. *IEEE Transactions on Intelligent Transportation Systems*, 16(6):3430–3439.

Liu, H., Manzoor, A., Wang, C., Zhang, L., and Manzoor, Z. (2020a). The covid-19 outbreak and affected countries stock markets response. *International journal of environmental research and public health*, 17(8):2800.

Liu, X., Gao, D., and Shen, G. (2020b). Conditional random fields with least absolute shrinkage and selection operator to classifying the barley genes based on expression level affected by the fungal infection. *Journal of Computational Biology*, 27(11):1581–1594.

Mazur, M., Dang, M., and Vega, M. (2021). Covid-19 and the march 2020 stock market crash. evidence from s&p1500. *Finance research letters*, 38:101690.

Moskvina, V. and Zhigljavsky, A. (2003). An algorithm based on singular spectrum analysis for change-point detection. *Communications in Statistics-Simulation and Computation*, 32(2):319–352.

Poskitt, D. S. (2020). On singular spectrum analysis and stepwise time series reconstruction. *Journal of Time Series Analysis*, 41(1):67–94.

Razali, N. M., Wah, Y. B., et al. (2011). Power comparisons of shapiro-wilk, kolmogorov-smirnov, lilliefors and anderson-darling tests. *Journal of statistical modeling and analytics*, 2(1):21–33.

Reid, S., Tibshirani, R., and Friedman, J. (2016). A study of error variance estimation in lasso regression. *Statistica Sinica*, pages 35–67.

Riedmiller, M. and Braun, H. (1993). A direct adaptive method for faster backpropagation learning: The rprop algorithm. In *IEEE international conference on neural networks*, pages 586–591. IEEE.

Rua, G. and Tito, M. D. (2024). Tapping the brakes the effect of the 2023 united auto workers strike on economic activity. Technical report, Board of Governors of the Federal Reserve System (US).

Shaphiro, S. and Wilk, M. (1965). An analysis of variance test for normality. *Biometrika*, 52(3):591–611.

Sun, Y., Phillips, P. C., and Jin, S. (2008). Optimal bandwidth selection in heteroskedasticity–autocorrelation robust testing. *Econometrica*, 76(1):175–194.

Tibshirani, R. (1996). Regression shrinkage and selection via the lasso. *Journal of the Royal Statistical Society Series B: Statistical Methodology*, 58(1):267–288.

Vautard, R. and Ghil, M. (1989). Singular spectrum analysis in nonlinear dynamics, with applications to paleoclimatic time series. *Physica D: Nonlinear Phenomena*, 35(3):395–424.

Wahlberg, B., Rojas, C. R., and Annergren, M. (2011). On l 1 mean and variance filtering. In *2011 Conference Record of the Forty Fifth Asilomar Conference on Signals, Systems and Computers (ASILOMAR)*, pages 1913–1916. IEEE.

Wang, Y. (1998). Smoothing spline models with correlated random errors. *Journal of the American Statistical Association*, 93(441):341–348.

ZOU, H., HASTIE, T., and TIBSHIRANI, R. (2007). On the "degrees of freedom" of the lasso. *The Annals of Statistics*, 35(5):2173–2192.